ADVANCED ELECTRONIC MATERIALS
www.advelectronicmat.de

Will We See Gigahertz Organic Transistors?

*Hagen Klauk**

Despite the many advances in the materials and technology of organic transistors, the highest transit frequency reported for organic transistors has not been improved for more than half a decade and remains far below 1 GHz. One reason is that most contributions to the field have traditionally focused on parameters that have little or no impact on the high-frequency performance of organic transistors. By analyzing the fundamental equations for the transit frequency and the effective (or apparent) carrier mobility, the requirements under which organic transistors can be expected to show a transit frequency of 1 GHz are reiterated. Not surprisingly, it is found that the critical parameter in this quest is not the charge-carrier mobility in the organic semiconductor layer, but the contact resistance, along with the channel length and the parasitic gate-to-contact overlaps.

1. Introduction

Organic thin-film transistors (TFTs) are field-effect transistors in which the semiconductor is a thin layer of conjugated organic molecules. Organic TFTs can typically be fabricated at relatively low process temperatures and thus not only on glass substrates, but also on plastics and paper, which makes organic TFTs potentially useful for flexible and stretchable electronics applications, such as rollable active-matrix displays and conformable sensor arrays.

An important TFT performance parameter is the unity-current-gain cutoff (or transit) frequency f_T, which is the highest frequency at which the transistor is able to amplify electrical signals

$$f_T = f\left(\frac{|i_D|}{|i_G|} = 1\right) = \frac{g_m}{2\pi C_G} \tag{1}$$

where i_D is the small-signal drain current (given as $i_D = g_m \cdot v_{GS}$, where g_m is the small-signal transconductance and v_{GS} is the small-signal gate–source voltage), i_G is the small-signal gate current (given as $i_G = j\, 2\pi\, f\, C_G v_{GS}$,[1] where j is the imaginary unit and f is the frequency), and C_G is the gate capacitance that includes the intrinsic contribution from the overlap of the gate electrode and the gate-field-induced charge-carrier channel in the semiconductor and the parasitic contributions from the overlap of the gate electrode and the source and drain contacts. By approximating the gate capacitance C_G as the sum of the geometric gate-to-channel and gate-to-contact capacitances, by assuming the same unit-area capacitance for the intrinsic and the parasitic capacitances, and by deriving the transconductance as $g_m = \partial I_D/\partial V_{GS}$ for the linear regime of transistor operation (i.e., for $V_{DS} < V_{GS} - V_{th}$, where V_{DS} is the large-signal drain–source voltage, V_{GS} is the large-signal gate–source voltage, and V_{th} is the threshold voltage), Equation (1) can be written as

$$f_T = \frac{\mu_{eff}\, V_{DS}}{2\pi L(L + L_{ov,GS} + L_{ov,GD})} \tag{2}$$

where μ_{eff} is the effective (or apparent) carrier mobility, L is the channel length, and $L_{ov,GS}$ and $L_{ov,GD}$ are the parasitic gate-to-source and gate-to-drain overlaps.

2. Results and Discussion

Solutions to Equation (2) for effective mobilities (μ_{eff}) of 1 and 10 $cm^2\ V^{-1}\ s^{-1}$, drain–source voltages (V_{DS}) of 1 and 10 V, and channel lengths (L) and gate overlaps ($L_{ov} = L_{ov,GS} = L_{ov,GD}$) ranging from 0.05 to 10 µm are plotted in **Figure 1**. Figure 1 suggests that transit frequencies of 1 GHz are indeed feasible for realistic effective carrier mobilities (≤10 $cm^2\ V^{-1}\ s^{-1}$) and realistic supply voltages (≤10 V), but only if the channel length and gate overlaps are smaller than 1 µm. If the critical TFT dimensions are greater than 1 µm, either unrealistically high mobilities or unrealistically large supply voltages would be required. For example, for $L = L_{ov}$ = 2 µm, i.e., for dimensions accessible by standard photolithography, an effective carrier mobility of 75 $cm^2\ V^{-1}\ s^{-1}$ would be required to achieve a transit frequency of 1 GHz at a drain–source voltage of 10 V. Even if self-alignment between the gate electrode and the source and drain contacts was employed to eliminate the parasitic gate overlaps ($L_{ov} = L_{ov,GS} = L_{ov,GD} = 0$), the effective carrier mobility required for f_T = 1 GHz at V_{DS} = 10 V and L = 2 µm is still 25 $cm^2\ V^{-1}\ s^{-1}$. Considering that the effective mobilities of organic TFTs are currently no greater than about 10 $cm^2\ V^{-1}\ s^{-1}$,[2–5] it appears that gigahertz organic TFTs will require critical dimensions below 1 µm.

But how realistic are effective carrier mobilities of 10 $cm^2\ V^{-1}\ s^{-1}$ or even 1 $cm^2\ V^{-1}\ s^{-1}$ in submicron organic TFTs? Of the more than 100 papers published to date on submicrometer-channel-length organic TFTs, only one has reported an effective mobility greater than 1 $cm^2\ V^{-1}\ s^{-1}$ (1.8 $cm^2\ V^{-1}\ s^{-1}$, at a channel length of 0.7 µm).[6] The reason is that at such small channel lengths, the transconductance and hence the effective carrier mobility are limited by the contact resistance, which,

Dr. H. Klauk
Max Planck Institute for Solid State Research
Heisenbergstr. 1, 70569 Stuttgart, Germany
E-mail: H.Klauk@fkf.mpg.de

The ORCID identification number(s) for the author(s) of this article can be found under https://doi.org/10.1002/aelm.201700474.

DOI: 10.1002/aelm.201700474

unlike the channel resistance, is independent of the channel length, so that the effective mobility decreases with decreasing channel length. For the linear regime of transistor operation ($V_{DS} < V_{GS} - V_{th}$), the relation between the effective carrier mobility μ_{eff} and the channel length L can be written as[7,8]

$$\mu_{eff} = \frac{\mu_0}{1 + \frac{\mu_0}{L} R_C W C_{diel} \left(V_{GS} - V_{th} - \frac{V_{DS}}{2} \right)} \tag{3}$$

where μ_0 is the intrinsic channel mobility (i.e., the carrier mobility in the absence of any contact resistance), R_C is the contact resistance (defined here as the sum of the source resistance and the drain resistance, i.e., $R_C = R_S + R_D$, and assumed to be Ohmic, i.e., independent of the voltage drop across the contacts), W is the channel width, and C_{diel} is the gate-dielectric capacitance per unit area. Solutions to Equation (3) for various intrinsic channel mobilities (μ_0), channel-width-normalized contact resistances ($R_C \cdot W$), and channel lengths (L) are plotted in **Figure 2**. The term $C_{diel}(V_{GS} - V_{th} - V_{DS}/2)$ was set to 10^{-6} As cm^{-2}, which is a typical value for transistors with conventional gate dielectrics. (For electrolyte-gated transistors, the value is typically in the range of 10^{-5} to 10^{-4} As cm^{-2}.[9])

Hagen Klauk received a Diplom-Ingenieur degree in electrical engineering from Chemnitz University of Technology, Germany, in 1995 and a Ph.D. degree in electrical engineering from the Pennsylvania State University in 1999. From 2000 to 2005 he was a Technical Staff member at Infineon Technologies in Erlangen, Germany. Since 2005 he has been head of the Organic Electronics group at the Max Planck Institute for Solid State Research in Stuttgart, Germany.

As a side note: According to Equation (3), the effective carrier mobility (μ_{eff}) decreases with increasing gate–source voltage (V_{GS}). The reason for this perhaps somewhat counterintuitive behavior becomes apparent in **Figure 3** where solutions to Equation (3) are plotted for various width-normalized contact

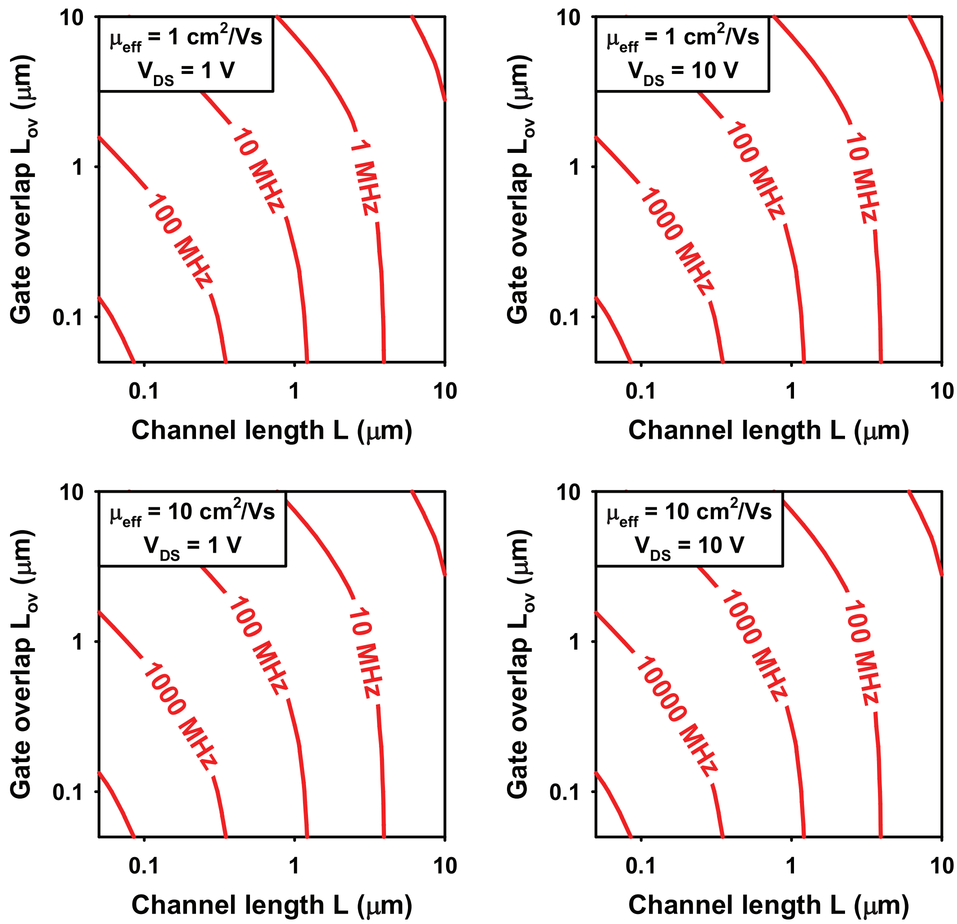

Figure 1. Contour plots showing the transit frequency (f_T) calculated using Equation (2) for various effective mobilities (μ_{eff}), drain–source voltages (V_{DS}), channel lengths (L), and gate overlaps ($L_{ov} = L_{ov,GS} = L_{ov,GD}$). For realistic effective mobilities (≤10 cm^2 V^{-1} s^{-1}) and voltages (≤10 V), gigahertz organic TFTs will require critical dimensions below 1 µm.

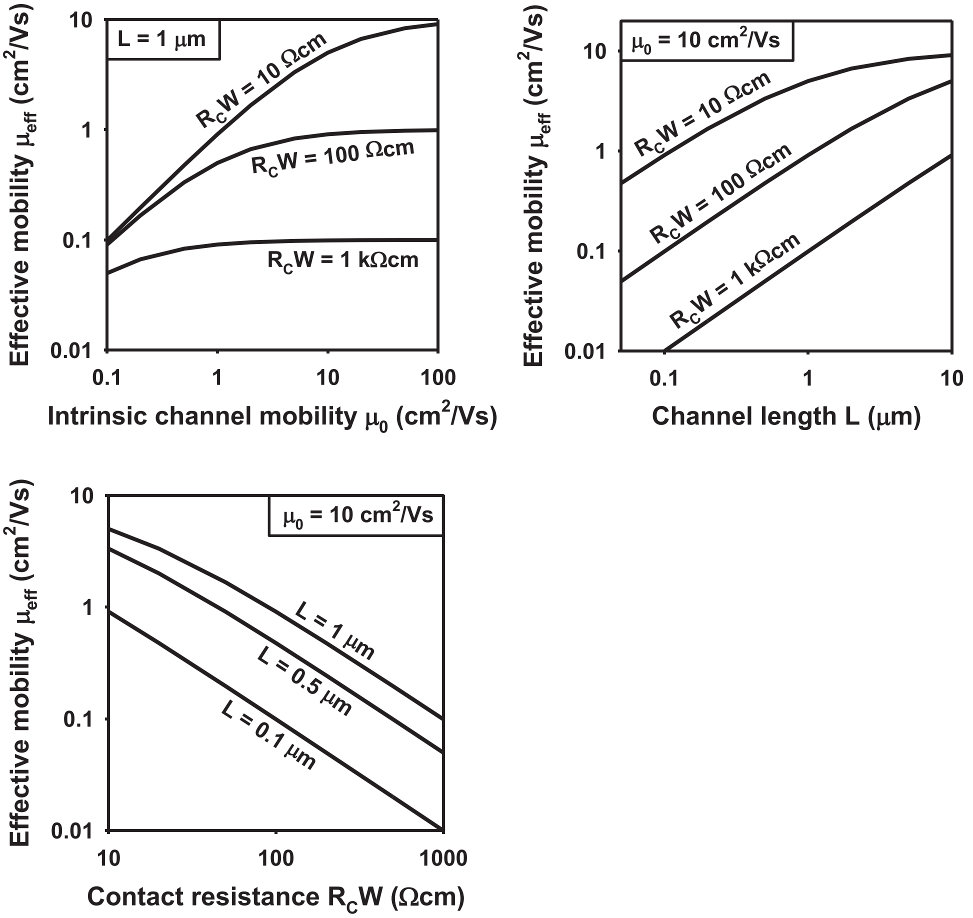

Figure 2. Effective carrier mobility (μ_{eff}) calculated using Equation (3) for various intrinsic channel mobilities (μ_0), channel lengths (L), and channel-width-normalized contact resistances ($R_C \cdot W$). The term $C_{\text{diel}}(V_{GS} - V_{th} - V_{DS}/2)$ was set to 10^{-6} As cm^{-2}. Effective carrier mobilities greater than 1 cm^2 V^{-1} s^{-1} at submicron channel lengths require a contact resistance below 100 Ωcm, regardless of the intrinsic channel mobility.

resistances ($R_C \cdot W$) and assuming the following parameters: $\mu_0 = 10$ cm^2 V^{-1} s^{-1}, $C_{\text{diel}} = 100$ nF cm^{-2}, $V_{\text{th}} = 0$ V, $V_{DS} = 0.1$ V, and $L = 10$ µm. As can be seen, the degree to which the effective carrier mobility depends on the gate–source voltage is strongly affected by the contact resistance: If the contact resistance is small, the effective carrier mobility is essentially independent of the applied gate–source voltage, as expected. However, in TFTs in which the contact resistance is large, significant fractions of the applied gate–source and drain–source voltages drop across the contact resistances, thus reducing the voltage drops across the semiconductor channel, which leads to a smaller-than-expected increase in drain current with increasing gate–source voltage and hence to a decrease in the transconductance and the effective mobility with increasing gate–source voltage.

Figure 2 shows that for small channel lengths, the effective carrier mobility drops significantly below the intrinsic channel mobility, especially when the contact resistance is large.[7] For channel lengths below 1 µm, an effective carrier mobility above 1 cm^2 V^{-1} s^{-1} can be achieved only if the contact resistance is smaller than 100 Ωcm, regardless of the intrinsic channel mobility. The second requirement for gigahertz organic TFTs (in addition to critical dimensions around or below 1 µm) is thus a contact resistance of less than 100 Ωcm. Note that achieving an effective carrier mobility of 10 cm^2 V^{-1} s^{-1} at a channel length of 1 µm or less would require an even smaller contact resistance of less than 10 Ωcm, regardless of the intrinsic channel mobility.

So how realistic is a contact resistance below 100 Ωcm in organic TFTs? Of the 300 papers to date discussing contact-resistance measurements on organic TFTs, only two have reported a contact resistance below 100 Ωcm. One of these is by Braga et al. who measured contact resistances as small as 1 Ωcm in electrolyte-gated polymer TFTs.[10] The authors argued that these very small contact resistances result from electrochemical doping of the semiconductor by ions that drift or diffuse from the electrolyte into the semiconductor layer. If this is the case, the result confirms the beneficial effect of doping for reducing the contact resistance of organic TFTs,[11,12] even though electrolyte-gating is unlikely to be a useful gating concept for gigahertz devices, since it relies on the inherently slow transport of ions in the electrolyte and since ionic doping of the semiconductor in the channel region will make it impossible to turn the transistors off with the gate field, rendering them useless for applications in digital circuits and active matrices. For doping to be a suitable approach to reducing the contact resistance in organic TFTs, the doping must be area-selective, i.e., limited to the contact regions.[11–13] The only other paper to

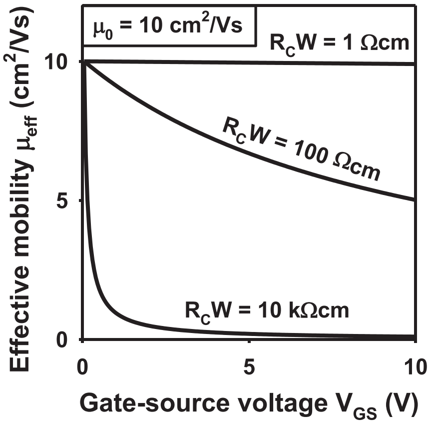

Figure 3. In TFTs in which the contact resistance ($R_C \cdot W$) is large, significant fractions of the applied gate–source and drain–source voltages drop across the contact resistances, and, as a result, the effective carrier mobility (μ_{eff}) calculated using Equation (3) shows a strong dependence on the gate–source voltage (V_{GS}). For the calculations, the following parameters were used: $\mu_0 = 10$ cm^2 V^{-1} s^{-1}, $C_{diel} = 100$ nF cm^{-2}, $V_{th} = 0$ V, $V_{DS} = 0.1$ V, $L = 10$ µm.

date reporting a contact resistance below 100 Ωcm in organic TFTs is by Stadlober et al. who measured a contact resistance of 80 Ωcm in pentacene TFTs fabricated in the inverted coplanar (bottom-gate, bottom-contact) device architecture with an SiO_2 gate dielectric and Au source/drain contacts covered with a thin layer of AuO_x produced by a UV/ozone treatment.[14] The authors found that the UV/ozone-grown AuO_x layer induces a more favorable thin-film morphology of the vacuum-deposited pentacene that leads to better continuity of the pentacene across the contact edges and thereby to a smaller contact resistance, similar to Au contacts covered with a functional thiol layer.[15] On the one hand, these results suggest that contact resistances below 100 Ωcm in organic TFTs are indeed feasible. On the other hand, the small number of publications in which a contact resistance below 100 Ωcm has been reported indicates that this target is not easily achieved.

By combining Equations (2) and (3), the following equation for the transit frequency can be obtained

$$f_T = \frac{\mu_0}{1 + \frac{\mu_0}{L} R_C W C_{diel} \left(V_{GS} - V_{th} - \frac{V_{DS}}{2} \right)} \frac{V_{DS}}{2\pi L (L + L_{ov,GS} + L_{ov,GD})} \quad (4)$$

Solutions to Equation (4) for various channel lengths (L), drain–source voltages (V_{DS}), intrinsic channel mobilities (μ_0), and width-normalized contact resistances ($R_C \cdot W$) are plotted in **Figure 4**. For simplicity, the parasitic gate overlaps are assumed to be zero ($L_{ov} = L_{ov,GS} = L_{ov,GD} = 0$) and the term $C_{diel}(V_{GS} - V_{th} - V_{DS}/2)$ was again set to 10^{-6} As cm^{-2}. Figure 4 shows that a transit frequency of 1 GHz at a drain–source voltage of 10 V will require a contact resistance no greater than 10 Ωcm in combination with an intrinsic channel mobility of at least 20 cm^2 V^{-1} s^{-1} if the channel length is 1 µm, or a contact resistance no greater than 100 Ωcm if the channel length is 0.1 µm.

Figure 4 illustrates the inherent tradeoff between the channel length and the requirement for the contact resistance: Reducing the channel length from 1 to 0.1 µm relaxes the contact resistance requirement from 10 to 100 Ωcm (at a drain–source voltage of 10 V). Note that this tradeoff cannot be avoided by increasing the intrinsic channel mobility: Even for an infinitely large intrinsic channel mobility, the contact resistance cannot be greater than 10 Ωcm if a transit frequency of 1 GHz is to be achieved at a drain–source voltage of 10 V with a channel length of 1 µm (and it cannot be greater than 100 Ωcm if 1 GHz is to be achieved at 10 V with $L = 0.1$ µm). Also note that these are the values for zero gate-to-contact overlap; if the parasitic gate overlaps are greater than zero, the contact resistance needs to be even smaller to offset the parasitic capacitance.

To further illustrate this critical tradeoff between the channel length and the contact resistance requirement, we rearrange Equation (2) to calculate the effective carrier mobility required for a certain transit frequency as a function of channel length and drain–source voltage and Equation (3) to calculate the contact resistance required to achieve this effective mobility

$$\mu_{eff} = \frac{2\pi L (L + L_{ov,GS} + L_{ov,GD}) f_T}{V_{DS}} \quad (5)$$

$$R_C W = \left(\frac{\mu_0}{\mu_{eff}} - 1 \right) \frac{L}{\mu_0 C_{diel} \left(V_{GS} - V_{th} - \frac{V_{DS}}{2} \right)} \quad (6)$$

Solutions to Equations (5) and (6) for a transit frequency of 1 GHz and drain–source voltages of 10 and 1 V are plotted in **Figure 5**, again assuming $L_{ov} = 0$ and $C_{diel}(V_{GS} - V_{th} - V_{DS}/2) = 10^{-6}$ As cm^{-2}. The intrinsic channel mobility was set to 10^4 cm^2 V^{-1} s^{-1}. Figure 5 confirms that reducing the channel length (e.g., from 1 to 0.1 µm) substantially softens the requirements for the effective carrier mobility and the contact resistance.

The key result to be taken from Figures 4 and 5 is that at the channel lengths required for gigahertz TFTs (i.e., $L \leq 1$ µm; see Figure 1), the transit frequency is essentially unaffected by the intrinsic channel mobility and is instead determined almost entirely by the contact resistance. If transit frequencies of 1 GHz in organic TFTs are to become a reality, the focus of future work thus needs to be shifted from increasing the carrier mobility to reducing the contact resistance. If the focus remains on large carrier mobilities, as it has been for the past decade, gigahertz organic transistors will forever remain a dream. In fact, many of the ultrahigh organic-TFT mobilities reported in recent years have likely come at the expense of a larger contact resistance, which means they have probably led to smaller, rather than larger, transit frequencies. Reducing the contact resistance of organic TFTs to 10 Ωcm is certainly a tall order and may require some creativity and unconventional approaches (aside from being less prestigious than claiming mobilities of 50 or 100 cm^2 V^{-1} s^{-1}), but it is by no means impossible.

In 2016, Perinot et al. reported a transit frequency of 20 MHz measured on a polymer TFT with a channel length of 1.75 µm, gate overlaps of 3 µm, and a gate-dielectric capacitance of 6.3 nF cm^{-2} at a gate–source voltage of 30 V.[16] Solutions to Equation (4) calculated using these parameters

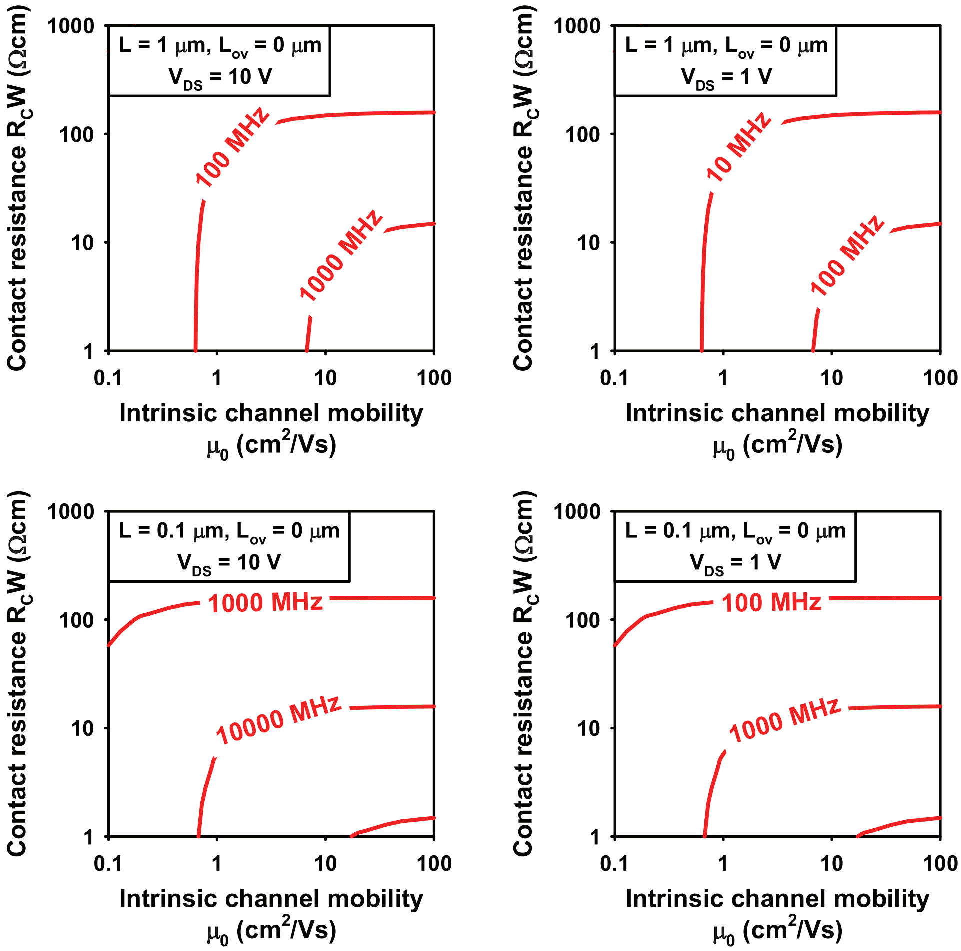

Figure 4. Contour plots showing the transit frequency (f_T) calculated using Equation (4) for various channel lengths (L), drain–source voltages (V_{DS}), intrinsic channel mobilities (μ_0), and width-normalized contact resistances ($R_C \cdot W$). The gate overlaps are assumed to be zero ($L_{ov} = L_{ov,GS} = L_{ov,GD} = 0$) and the term $C_{diel}(V_{GS} - V_{th} - V_{DS}/2)$ was set to 10^{-6} As cm^{-2}. A transit frequency of 1 GHz at a drain–source voltage of 10 V requires a contact resistance of 10 Ωcm if the channel length is 1 µm, or a contact resistance of 100 Ωcm if the channel length is 0.1 µm.

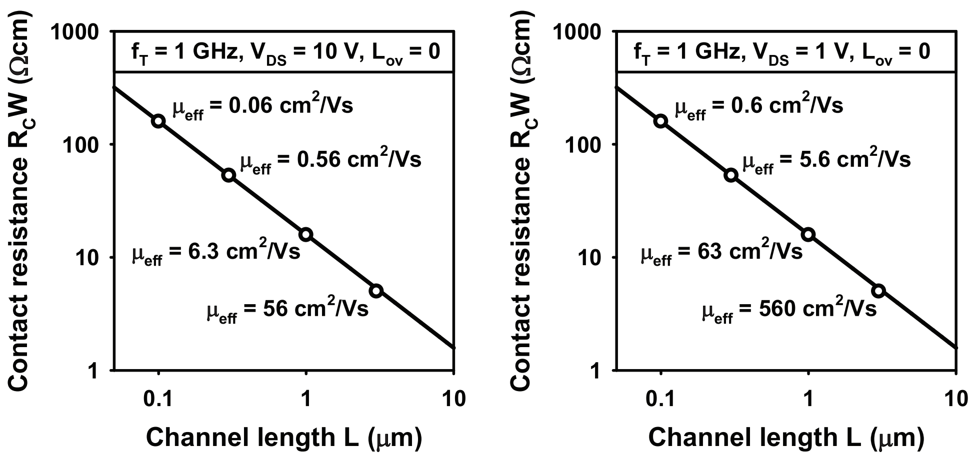

Figure 5. Requirements for the effective carrier mobility (μ_{eff}) and the channel-width-normalized contact resistance ($R_C \cdot W$) as a function of the channel length (L), calculated using Equations (5) and (6) for two different drain–source voltages (V_{DS}). The gate overlaps are assumed to be zero ($L_{ov} = 0$) and the term $C_{diel}(V_{GS} - V_{th} - V_{DS}/2)$ was set to 10^{-6} As cm^{-2}. Reducing the channel length will substantially alleviate the requirements for the effective carrier mobility and the contact resistance.

(and assuming a threshold voltage of 0 V and a drain–source voltage of 30 V) are plotted in **Figure 6**a, showing that for these parameters, a transit frequency of 1 GHz would require an intrinsic channel mobility of 30 cm^2 V^{-1} s^{-1}. Given that mobilities of 30 cm^2 V^{-1} s^{-1} are out of reach, solutions to Equation (4) calculated using $L = L_{ov} = 0.2$ µm, $C_{diel} = 50$ nF cm^{-2}, $V_{GS} = V_{DS} = 10$ V, and $V_{th} = 0$ V are plotted in Figure 6b. As can be seen, for these smaller TFT dimensions, a transit frequency of 1 GHz is feasible for a much more modest intrinsic channel mobility of 1 cm^2 V^{-1} s^{-1}, provided the contact resistance is around 50 Ωcm.

According to ref. [16], the TFTs on which the transit frequency of 20 MHz was measured have an effective carrier mobility (μ_{eff}) of 0.13 cm^2 V^{-1} s^{-1} and a contact resistance ($R_C \cdot W$) of 7.3 kΩ cm. From these values, the intrinsic channel mobility (μ_0) in the linear regime is estimated using Equation (3) to be about 1 cm^2 V^{-1} s^{-1}. In Figure 6a,b, a data point has been included to illustrate this particular set of $\mu_0 = 1$ cm^2 V^{-1} s^{-1} and $R_C \cdot W = 7.3$ kΩ cm. For this combination of μ_0 and $R_C \cdot W$, a transit frequency of 7 MHz is calculated using Equation (4), which is a factor of three smaller than the measured transit frequency of 20 MHz. The reason for this discrepancy is unknown, but it is important to remember that in deriving Equation (3), the contact resistance was assumed to be linear, i.e., independent of the voltage drops across the contacts. In reality, the contact resistance must be expected to have a nonlinear component. This nonlinearity is not easily captured in simple equations like those employed here, but it can be captured by modeling the transistor as an equivalent network of linear and nonlinear circuit elements and solving the current–voltage equations using a circuit simulator.[17] In ref. [17], it is shown that in TFTs fabricated in the staggered device architecture, such as those reported in ref. [16], the nonlinear contributions to the contact resistance lead to a larger transconductance and hence larger transit frequency compared to a transistor with purely linear contact resistances. This may explain the discrepancy between the transit frequency predicted using Equation (4) and the measured transit frequency reported in ref. [16]. It will also alleviate the decrease of the effective carrier mobility with increasing gate–source voltage seen in Figure 3. In this sense, the inherent nonlinearity of the contact resistance is actually helpful in achieving higher transit frequencies.

Returning to the question raised in the title: Gigahertz organic TFTs are clearly feasible, but only if the focus of future efforts is shifted from the pointless ultrahigh-mobility hype of recent years to a more target-oriented emphasis on those TFT parameters that actually benefit the transit frequency: channel length, parasitic overlap, and contact resistance.

3. Additional Remarks

1. Since the transit frequency f_T is a small-signal parameter, the results above relate directly to analog circuits. The dynamic performance of digital circuits, in which the transistors are switching large signals, is characterized by the stage delay τ and the equivalent frequency $f_{eq} = 1/(2\tau)$. The equivalent frequency of a digital circuit is necessarily smaller than the transit frequency of the individual transistors: for example, ring oscillators based on organic TFTs with a channel length of 1 µm and gate overlaps of 5 µm, for which a transit frequency of 2.2 MHz was determined by scattering-parameter measurements at a drain–source voltage 2.5 V,[18] operated with a stage delay of 550 ns at a supply voltage of 2.5 V,[19] which corresponds to an equivalent frequency of 0.9 MHz, so the ratio between the equivalent frequency f_{eq} and the transit frequency f_T is ≈0.4 in this case. Across various field-effect-transistor technologies, the ratio f_{eq}/f_T is usually in the range of 0.4–0.6,[20] which means that digital circuits based on transistors with a transit frequency of 1 GHz are expected to have an equivalent frequency of ≈0.5 GHz and a stage delay of ≈1 ns.

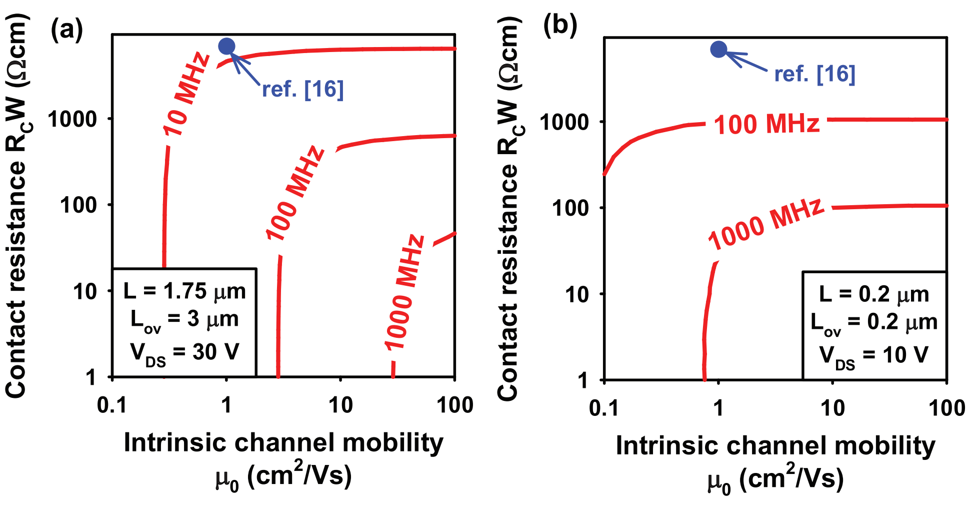

Figure 6. a) Contour plot showing the transit frequency (f_T) calculated using Equation (4) for the TFT parameters published in ref. [16] ($L = 1.75$ µm, $L_{ov} = 3$ µm, $C_{diel} = 6.3$ nF cm^{-2}, $V_{GS} = 30$ V) and assuming $V_{th} = 0$ V and $V_{DS} = 30$ V. The data point at $\mu_0 = 1$ cm^2 V^{-1} s^{-1} and $R_C \cdot W = 7.3$ kΩ cm reflects the intrinsic channel mobility and the contact resistance of the TFTs in ref. [16]. b) Contour plot showing the transit frequency (f_T) calculated using Equation (4) for an aggressively scaled version of the TFT reported in ref. [16] ($L = L_{ov} = 0.2$ µm, $C_{diel} = 50$ nF cm^{-2}, $V_{GS} = V_{DS} = 10$ V, $V_{th} = 0$ V). For these TFT dimensions, an intrinsic channel mobility of 1 cm^2 V^{-1} s^{-1} is sufficient for a transit frequency of 1 GHz, provided the contact resistance is below 100 Ωcm.

2. The total resistance of a field-effect transistor can be considered as the sum of the contact resistance and the resistance of the gate-induced charge-carrier channel ($R_{total} = R_C + R_{channel}$). The width-normalized channel resistance in the linear regime of transistor operation can be written as

$$R_{channel}\, W = \frac{L}{\mu_0\, C_{diel}\left(V_{GS} - V_{th} - \frac{V_{DS}}{2}\right)} \tag{7}$$

For $\mu_0 = 1\ cm^2\ V^{-1}\ s^{-1}$ and $C_{diel}(V_{GS} - V_{th} - V_{DS}/2) = 10^{-6}$ As cm^{-2}, we thus have $R_{channel} \cdot W = 100\ \Omega cm$ when $L = 1\ \mu m$ and $R_{channel} \cdot W = 10\ \Omega cm$ when $L = 0.1\ \mu m$. These values can be compared to the maximum contact resistance required for a transit frequency of 1 GHz: For $L = 1\ \mu m$, $L_{ov} = 0$, $V_{DS} = 10$ V, and $f_T = 1$ GHz, the contact resistance needs to be 10 Ωcm (see Figure 5), so in this case, the contact resistance would account for less than 10% of the total device resistance. For $L = 0.1\ \mu m$, $L_{ov} = 0$, $V_{DS} = 10$ V, and $f_T = 1$ GHz, the contact resistance can be as large as 100 Ωcm, so the contact resistance may account for up to 90% of the total device resistance. Such a device would display a severe nonlinearity in the output characteristics (I_D vs V_{DS}) at small drain–source voltages.[12] To alleviate this undesirable nonlinearity, the contact resistance would need to be reduced to about 10 Ωcm.

3. For TFTs in which the charge carriers are injected into and extracted from the semiconductor layer across an extended area above or below the source and drain contacts (as opposed to TFTs in which the injection and extraction occur only along the leading edge of the contact), the contact behavior can be described by the current-crowding model[21] and an area-normalized contact resistivity (or specific contact resistance) ρ_C can be introduced that is related to the width-normalized contact resistance $R_C \cdot W$ in the linear regime of transistor operation approximately as follows[22]

$$\rho_C \approx (R_C\, W)^2\, \mu_0\, C_{diel}\left(V_{GS} - V_{th} - \frac{V_{DS}}{2}\right) \tag{8}$$

Solutions to Equation (8) for intrinsic channel mobilities (μ_0) of 1 and 10 $cm^2\ V^{-1}\ s^{-1}$ are plotted in **Figure 7**. The term $C_{diel}(V_{GS} - V_{th} - V_{DS}/2)$ was again set to 10^{-6} As cm^{-2}. As can be seen, a contact resistance of 100 Ωcm (which according to Figure 5 is the requirement for a transit frequency of 1 GHz at $L = 0.1\ \mu m$, $L_{ov} = 0$, and $V_{DS} = 10$ V) translates into a contact resistivity of 0.1 Ωcm^2 if $\mu_0 = 10\ cm^2\ V^{-1}\ s^{-1}$ and 0.01 Ωcm^2 if $\mu_0 = 1\ cm^2\ V^{-1}\ s^{-1}$, similar to the results of calculations performed by Risteska et al.[8] Contact resistivities of 0.1 Ωcm^2 have already been reported for organic TFTs.[8,12,22]

4. Thin-film transistors can be fabricated in the staggered or the coplanar device architecture. The answer to the question which of these two architectures will ultimately provide the smaller contact resistance depends on a large number of parameters and considerations.[23,24]

5. For both device architectures, the contact resistance usually displays a monotonic decrease with increasing gate–source voltage.[25] In staggered TFTs without contact doping, the contact resistance has been shown to increase monotonically with decreasing gate overlap if the gate overlap is smaller than the transfer length,[26] but the extent to which this increase in contact resistance with decreasing gate overlap affects the transit frequency may be less dramatic than expected.[17]

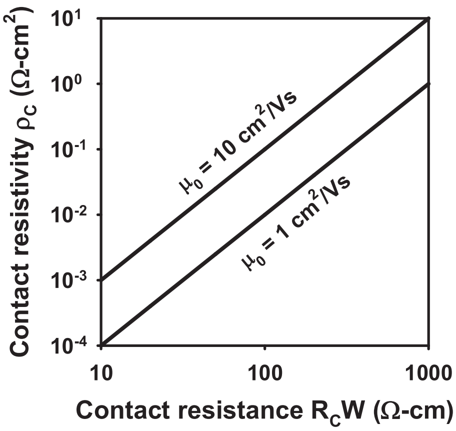

Figure 7. Contact resistivity (ρ_C) calculated using Equation (8) as a function of the channel-width-normalized contact resistance ($R_C \cdot W$) for two different intrinsic channel mobilities (μ_0). The term $C_{diel}(V_{GS} - V_{th} - V_{DS}/2)$ was set to 10^{-6} As cm^{-2}.

6. The contact resistance of inverted staggered (bottom-gate, top-contact) TFTs can be measured directly using Kelvin probe force microscopy.[27,28] Alternatively (and regardless of the device architecture) the contact resistance can be accessed indirectly, for example, using the transmission (or transfer) line method,[7,10–17,25,26] the gated four-probe method,[29,30] the gated van der Pauw method,[31] or by fitting the current–voltage characteristics of the transistors to an appropriate transistor model.[17]

7. For the solutions to Equations (4)–(6) plotted in Figures 4 and 5, the parasitic gate-to-source and gate-to-drain overlaps $L_{ov,GS}$ and $L_{ov,GD}$ were assumed to be zero. The fabrication of TFTs with zero gate overlap will generally require some form of self-alignment between the gate electrode and the source and drain contacts, which can be accomplished, for example, with the help of a backside exposure through the (optically transparent) substrate.[32] Submicrometer source–drain gaps can be fabricated with a variety of approaches, such as nanoimprint lithography,[14,32] laser processing,[16,33] gravure printing,[34] vertical TFT architectures,[35] stencil-mask lithography,[36] adhesion lithography,[37] and others.

8. Applying a drain–source voltage of 10 V to a TFT with a channel length of 0.1 µm will produce an electric field of 1 MV cm^{-1} in the semiconductor, which is likely to be close to the breakdown field of the semiconductor. The consequences of a prolonged application of such large electric fields to the organic semiconductor layer will need to be studied.

Conflict of Interest

The authors declare no conflict of interest.

Keywords

contact resistance, organic thin-film transistors, transit frequency

Received: September 28, 2017
Revised: November 22, 2017
Published online: January 25, 2018

[1] M. Kitamura, Y. Arakawa, *Jpn. J. Appl. Phys.* **2011**, *50*, 01BC01.
[2] H. Minemawari, T. Yamada, H. Matsui, J. Tsutsumi, S. Haas, R. Chiba, R. Kumai, T. Hasegawa, *Nature* **2011**, *475*, 364.
[3] J. Soeda, T. Okamoto, C. Mitsui, J. Takeya, *Org. Electron.* **2016**, *39*, 127.
[4] T. Hamai, S. Arai, H. Minemawari, S. Inoue, R. Kumai, T. Hasegawa, *Phys. Rev. Appl.* **2017**, *8*, 054011.
[5] E. G. Bittle, J. I. Basham, T. N. Jackson, O. D. Jurchescu, D. J. Gundlach, *Nat. Commun.* **2016**, *7*, 10908.
[6] H. Wang, C. Cheng, L. Zhang, H. Liu, Y. Zhao, Y. Guo, W. Hu, G. Yu, Y. Liu, *Adv. Mater.* **2014**, *26*, 4683.
[7] M. Marinkovic, D. Belaineh, V. Wagner, D. Knipp, *Adv. Mater.* **2012**, *24*, 4005.
[8] A. Risteska, K. Myny, S. Steudel, M. Nakamura, D. Knipp, *Org. Electron.* **2014**, *15*, 461.
[9] J. H. Cho, J. Lee, Y. Xia, B. Kim, Y. He, M. J. Renn, T. P. Lodge, C. D. Frisbie, *Nat. Mater.* **2008**, *7*, 900.
[10] D. Braga, M. Ha, W. Xie, C. D. Frisbie, *Appl. Phys. Lett.* **2010**, *97*, 193311.
[11] T. Minari, T. Miyadera, K. Tsukagoshi, Y. Aoyagi, H. Ito, *Appl. Phys. Lett.* **2007**, *91*, 053508.
[12] F. Ante, D. Kälblein, U. Zschieschang, T. W. Canzler, A. Werner, K. Takimiya, M. Ikeda, T. Sekitani, T. Someya, H. Klauk, *Small* **2011**, *7*, 1186.
[13] S. Choi, C. Fuentes-Hernandez, C.-Y. Wang, T. M. Khan, F. A. Larrain, Y. Zhang, S. Barlow, S. R. Marder, B. Kippelen, *ACS Appl. Mater. Interfaces* **2016**, *8*, 24744.
[14] B. Stadlober, U. Haas, H. Gold, A. Haase, G. Jakopic, G. Leising, N. Koch, S. Rentenberger, E. Zojer, *Adv. Funct. Mater.* **2007**, *17*, 2687.
[15] M. Kitamura, Y. Kuzumoto, Y. Arakawa, *Phys. Status Solidi C* **2013**, *10*, 1632.
[16] A. Perinot, P. Kshirsagar, M. A. Malvindi, P. P. Pompa, R. Fiammengo, M. Caironi, *Sci. Rep.* **2016**, *6*, 38941.
[17] A. Fischer, H. Zündorf, F. Kaschura, J. Widmer, K. Leo, U. Kraft, H. Klauk, *Phys. Rev. Appl.* **2017**, *8*, 054012.
[18] T. Zaki, R. Rödel, F. Letzkus, H. Richter, U. Zschieschang, H. Klauk, J. N. Burghartz, *IEEE Electron Device Lett.* **2013**, *34*, 520.
[19] U. Zschieschang, R. Hofmockel, R. Rödel, U. Kraft, M. J. Kang, K. Takimiya, T. Zaki, F. Letzkus, J. Butschke, H. Richter, J. N. Burghartz, H. Klauk, *Org. Electron.* **2013**, *14*, 1516.
[20] J.-O. Plouchart, J. Kim, N. Zamdmer, M. Sherony, Y. Tan, M. Yoon, M. Talbi, A. Ray, L. Wagner, in *2003 European Solid-State Circuits Conf. Technical Digest*, (Eds. J. Franca, R. Koch), IEEE Piscataway, NJ, USA, p. 357.
[21] T. J. Richards, H. Sirringhaus, *J. Appl. Phys.* **2007**, *102*, 094510.
[22] A. Hoppe, D. Knipp, B. Gburek, A. Benor, M. Marinkovic, V. Wagner, *Org. Electron.* **2010**, *11*, 626.
[23] M. Gruber, E. Zojer, F. Schürrer, K. Zojer, *Adv. Funct. Mater.* **2013**, *23*, 2941.
[24] K. Zojer, E. Zojer, A. Fernandez, M. Gruber, *Phys. Rev. Appl.* **2015**, *4*, 044002.
[25] D. J. Gundlach, L. Zhou, J. A. Nichols, T. N. Jackson, P. V. Necliudov, M. S. Shur, *J. Appl. Phys.* **2006**, *100*, 024509.
[26] F. Ante, D. Kälblein, T. Zaki, U. Zschieschang, K. Takimiya, M. Ikeda, T. Sekitani, T. Someya, J. N. Burghartz, K. Kern, H. Klauk, *Small* **2012**, *8*, 73.
[27] K. Seshadri, C. D. Frisbie, *Appl. Phys. Lett.* **2001**, *78*, 993.
[28] G. de Tournadre, F. Reisdorffer, R. Rödel, O. Simonetti, H. Klauk, L. Giraudet, *J. Appl. Phys.* **2016**, *119*, 125501.
[29] P. V. Pesavento, R. J. Chesterfield, C. R. Newman, C. D. Frisbie, *J. Appl. Phys.* **2004**, *96*, 7312.
[30] W. L. Kalb, F. Meier, K. Mattenberger, B. Batlogg, *Phys. Rev. B* **2007**, *76*, 184112.
[31] C. Rolin, E. Kang, J.-H. Lee, G. Borghs, P. Heremans, J. Genoe, *Nat. Commun.* **2017**, *8*, 14975.
[32] S. G. Higgins, B. V. O. Muir, G. Dell'Erba, A. Perinot, M. Caironi, A. J. Campbell, *Appl. Phys. Lett.* **2016**, *108*, 023302.
[33] S. G. Bucella, G. Nava, K. C. Vishunubhatla, M. Caironi, *Org. Electron.* **2013**, *14*, 2249.
[34] R. Kitsomboonloha, H. Kang, G. Grau, W. Scheideler, V. Subramanian, *Adv.Electron. Mater.* **2015**, *1*, 1500155.
[35] M. Uno, B.-S. Cha, Y. Kanaoka, J. Takeya, *Org. Electron.* **2015**, *20*, 119.
[36] U. Zschieschang, F. Letzkus, J. N. Burghartz, H. Klauk, *IEEE Trans. Nanotechnol.* **2017**, *16*, 837.
[37] J. Semple, G. Wyatt-Moon, D. G. Georgiadou, M. A. McLachlan, T. D. Anthopoulos, *IEEE Trans. Electron Devices* **2017**, *64*, 1973.